Air Oxidation at 600-800°C of Two Nanophase Co-50wt% Cu Alloys Prepared By Mechanical Alloying

J. Song*, G. Farnè°, Y. Niu*°, F. Gesmundo°, P. Matteazzi £ and G. Randi°

* *State Key Lab for Corrosion & Protection, Institute of Corrosion and Protection of Metals, Academia Sinica, Wencui Road 62, 110015 Shenyang (China)*
° *Dipartimento di Ingegneria Chimica, Università di Genova, 16129 Genova (Italy)*
£ *Dipartimento di Scienze e Tecnologie Chimiche, Università di Udine, Udine (Italy)*

(Received January 18, 2000; final form March 20, 2000)

ABSTRACT

The air oxidation of two two-phase cobalt-copper alloys prepared by mechanical alloying, containing approximately 50 wt%Cu but presenting two different grain sizes, has been studied at 600-800°C. The two alloys have been obtained by sintering a mixture of nanophase Co-Cu powders by hot isostatic pressing followed or not by an annealing at 800°C for 20 hr. Both alloys formed composite scales containing complex mixtures of copper and cobalt oxides associated with an internal oxidation of cobalt in a copper matrix. The kinetics of oxidation were close to parabolic at 600 and 700°C, but rather irregular at 800°C. Moreover, the oxidation rates of the two alloys were similar at 600°C, but the annealed alloy corroded more slowly at 700 and 800°C. On the whole, the scaling behavior of the two nanophase alloys was rather similar to that of an alloy of the same composition prepared by conventional casting techniques and thus presenting a much larger grain size. Thus, the very small grain size of the present alloys is not yet sufficient to produce an exclusive external oxidation of cobalt, as might be expected as a result of a possible faster diffusion of cobalt along grain boundaries in the alloy. The presence of large convolutions in the outermost CuO layer and the extensive spallation of the underlying Cu_2O layer are attributed to the accumulation of mechanical stresses in the scale due to the penetration of oxygen along the grain boundaries in the scale and to a reduction of the sample size associated with the increase in the alloy grain size with time during oxidation.

Key words: Co-Cu, mechanical alloying, two-phase, high temperature, oxidation

1. INTRODUCTION

Cobalt and copper have a small mutual solubility and do not form any intermediate phase /1/. Thus, Co-Cu alloys contain variable volume fractions of the two conjugated solid solutions presenting a widely different composition in most of their composition range. Two-phase alloys based on copper, including also Cu-Cr, Cu-Fe and Cu-Nb, are of increasing interest for their electric and magnetic properties and also because the presence of particles of the Cu-poor phase in a copper matrix improves their mechanical properties

°Correspondence: Dr. Y. Niu, Dipartimento di Ingegneria Chimica, Università di Genova, Fiera del Mare, Pad.D 16129 Genova (Italy). Fax: +39-010-3536028; Email: gesmundo@unige.it

considerably with respect to pure Cu, particularly when the alloys are nanophase /2,3/. In particular, they are also considered for electrical applications at rather high temperatures /3,4/, so that their oxidation resistance is also of concern. The air oxidation at 600-800°C of three Co-Cu alloys containing 25, 50 and 75 wt% copper and prepared by means of conventional casting techniques has been examined previously /5/. The present Co-Cu alloys have been prepared by mechanical alloying and thus have grain sizes for both phases much finer than those of the alloys examined previously. In addition, they contain a significantly more uniform phase distribution, generally difficult to achieve when using conventional methods. The aim of this paper is to examine the possible effects of a large reduction of the grain size of two-phase Co-Cu alloys on the various aspects of their scaling behavior at high temperatures, including the kinetics of oxidation and the properties of the corresponding scales and in particular to establish if this change in the alloy microstructure can produce a significant decrease of the critical cobalt content required to prevent the oxidation of copper in Co-Cu alloys.

2. EXPERIMENTAL

A cobalt-copper alloy with a nominal copper content of about 50 wt% was prepared by mechanical alloying. The starting materials were powders of copper (99.9%, particle size 50-120 μm) and cobalt (99.9%, particle size 45-140 μm). The synthesis of the nanophase Cu-50Co powders was performed in a high energy, high capacity planetary ball mill (MBN HEMILL 8). The elemental powders were introduced into a vial, together with carbon steel balls (with a powder-to ball ratio 1:8) using a glove box filled with argon. The vial had a volume of 50 cm^3 and was rotated clockwise at a speed of 650 rpm for an overall milling time of 8 h with 5 min stops every 15 min to avoid overheating of the sample. The vial, provided with an O-ring, was sealed, evacuated to 10^2 Pa and filled with argon. Bottom and top water cooling of the vial was employed, keeping the temperature rise of the vial walls low and allowing continuous milling without excessive heat effects. Powder consolidation was carried out by Hot Isostatic Pressing (HIP) at 550°C using a copper container. Part of this alloy was annealed at 800°C for 20 hours under 10^7 Pa, to study the extent of grain growth during oxidation and its possible effects on the corrosion kinetics. The annealed alloy is denoted ANMA Co-50Cu, while the original material is denoted ORMA Co-50Cu.

Figs. 1a-1c show the microstructures of the two-nanophase alloys plus that of the cast alloy with the same composition (Cast Co-50Cu). In agreement with the Co-Cu phase diagram, all alloys contain mixtures of the solid solution of cobalt in copper (α phase, light) and of copper in cobalt (β phase, dark). Part of the small dark islands present in the micrographs of ORMA Co-50Cu and ANMA Co-50Cu are pores but part are of cobalt oxide (CoO), formed during the preparation of the alloy due to the unavoidable presence of traces of oxygen. From a semiquantitative EDX analysis and a careful examination of the alloy microstructure the fraction of cobalt tied up as oxide is estimated to be about 15 % of the overall cobalt content, so that the concentration of active cobalt, i.e. of cobalt still present as a metal, is around 45 wt% rather than 50 wt%. According to the XRD analysis using the Warren-Averbach method, the average grain size of the two phases is about 22 nm for Cu and 12 nm for Co in ORMA Co-50Cu, while it is about 52 nm for Cu and 65 nm for Co in ANMA Co-50Cu. The particles of two components are larger than the corresponding grains, but they are still too fine to be visible under the SEM. ANMA Co-50Cu is more porous than ORMA Co-50Cu, very likely as a result of a volume reduction due to the increase of the particle size during annealing.

Samples about 1 mm thick and with a surface area of about 2-3 cm^2 were cut from the final ingots by means of a diamond-wheel saw, ground down to 600 grit emery paper, degreased and dried immediately before each test. Oxidation tests were carried out in air at 600, 700 and 800°C using a Cahn microbalance model 2000. Samples of ORMA Co-50Cu and ANMA Cu-50Cu alloys have been oxidized in air at 600-800°C, the former for 24 h, except at 800°C when the oxidation was too fast, and the latter for 16 h. In addition, two samples of ORMA Co-50Cu have been oxidized at 600°C for only 0.5 h and 1 h, respectively. The corroded samples

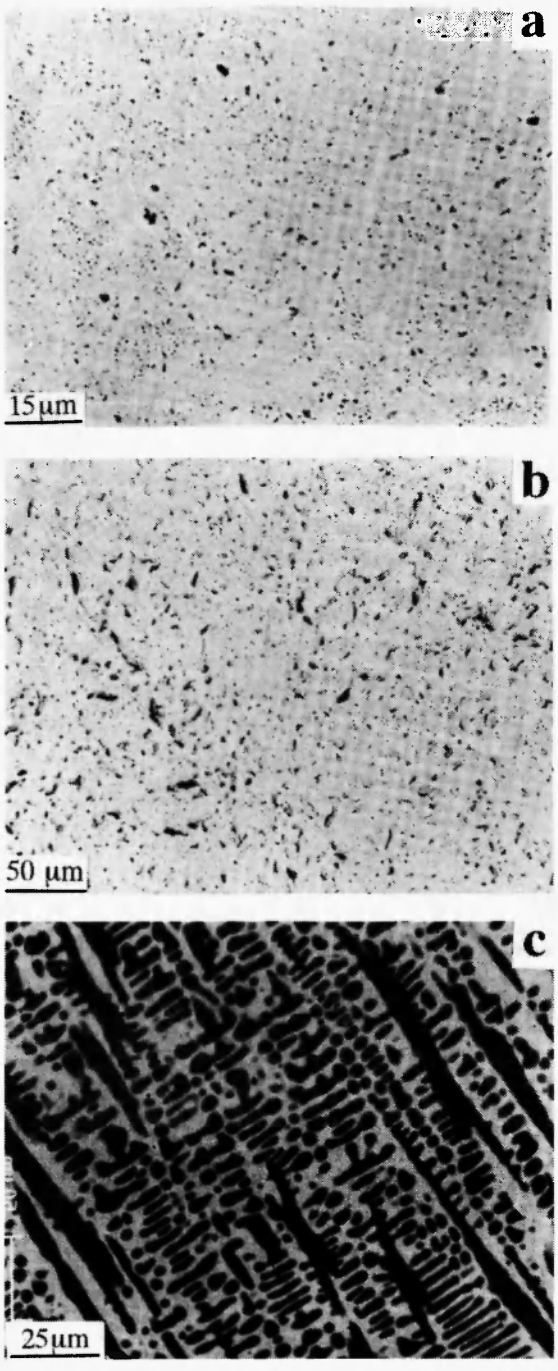

Fig. 1: Microstructures (SEM/BEI) of three two-phase Co-50wt%Cu alloys.
(1a) prepared by mechanical alloying followed by HIP (ORMA);
(1b) prepared by annealing ORMA Co-50Cu at 800°C for 20 h (ANMA);
(1c) prepared by conventional arc melting (Cast).

were examined by means of X-ray diffraction (XRD), scanning electron microscopy (SEM) and energy-dispersive X-ray microanalysis (EDX) to identify the corrosion products and to establish their composition and their spatial distribution within the scales.

3. RESULTS

3.1 Oxidation kinetics

The kinetics curves for the oxidation of the two MA Co-50Cu alloys at 600, 700 and 800°C are shown in Figs. 2a-2c, respectively, where they are compared with those of Cast Co-50Cu. For all alloys the oxidation rates increase with temperature, the largest effect occurring between 700 and 800°C. At 700 and 800°C the oxidation rates of ORMA Co-50Cu are higher that those of ANMA Co-50Cu, while at 600°C that of ORMA Co-50Cu is slightly lower that that of ANMA Co-50Cu. The oxidation of ORMA at 600°C and of ANMA Co-50Cu at 600-700°C follow the parabolic rate law to a reasonable approximation, even though the instantaneous parabolic rate constants, i.e. the slopes of the plots of the square of weight gain vs time, tend to change slightly with time. ORMA Co-50Cu at 700°C shows two main parabolic stages with a larger rate constant during the second stage of the oxidation. Finally, the oxidation of the two alloys at 800°C is rather irregular and involves three main periods, including an initial approximately parabolic stage followed by a sudden rate increase and then by a third stage close to parabolic for ANMA Co-50Cu but rather irregular (with an initial rate increase and then an approximately linear stage) for ORMA Co-50Cu. Approximate values of the parabolic rate constants calculated from appropriate sections of the kinetics curves are given in Table I together with the corresponding values for Cast Co-50Cu and the two pure metals /6,7/. In comparison with the cast alloy ORMA Co-50Cu oxidizes at a similar rate at 600°C, but larger at 700 and 800°C, while ANMA Co-50Cu oxidizes slightly more rapidly at 600°C, approximately at the same rate at 700°C and again more rapidly at 800°C.

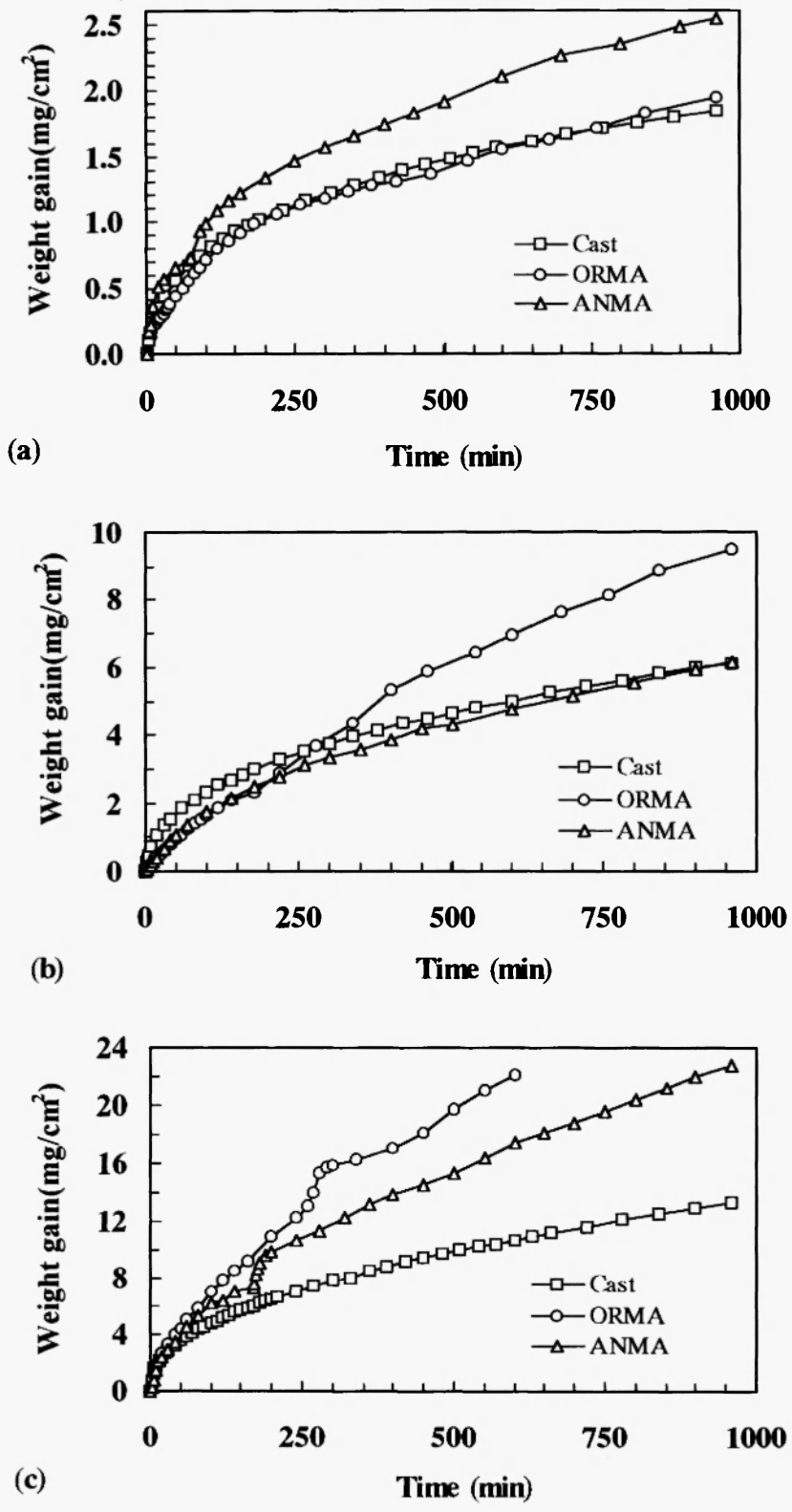

Fig. 2: Scaling kinetics of the three Co-50Cu alloys (ORMA, ANMA and Cast) oxidized in air at 600 (2a), 700 (2b) and 800°C (2c).

Table 1

Approximate parabolic rate constants ($g^2\ cm^{-4}\ s^{-1}$) for the air oxidation of pure Cu and Co and of three Co-50Cu alloys with different microstructures at 600-800°C

Temp. / Maters.		Co [a]	ORMA Co-50Cu	ANMA Co-50Cu	Cast Co-50Cu	Cu
600°C	initial average final	1.7×10^{-11}	6.5×10^{-11}	4.8×10^{-11}	9.3×10^{-11}	1.5×10^{-10} [b]
700°C	initial average final	5.9×10^{-11}	3.8×10^{-10} - 3.2×10^{-9}	3.6×10^{-10}	7.8×10^{-10} - 4.7×10^{-10}	1.2×10^{-9}
800°C	initial average final	2.7×10^{-10}	-	9.5×10^{-9}	2.8×10^{-9}	5.4×10^{-9}

(a): from Morin *et al.* /7/; (b): from Gesmundo *et al.* /6/

3.2 - Scale microstructure and composition

In all cases, the present alloys form complex external scales containing the oxides of both components, plus a region of internal oxidation of cobalt which is thicker for ANMA Co-50Cu than for ORMA Co-50Cu at same temperature (but for longer oxidation times). The outermost scale region formed under all conditions is always a thin layer of CuO. However, the details of the structure and composition of the external scales change with temperature and alloy structure as examined below by considering each condition separately.

ORMA Co-50Cu oxidized at 600°C (Figs. 3a-3b) shows a convoluted outermost layer of CuO containing about 1 at% cobalt (light gray), only about 2 μm thick, entirely detached from the underlying scale. Underneath this layer there is an inner region composed of CoO containing about 8 at% copper (gray), followed by a region of internal oxidation of cobalt. The outer zone of this layer is compact, while the inner zone is very porous. Figs. 4a shows a cross section of the scale grown on this alloy after oxidation at 600°C for only 0.5 h: the CuO layer is only partly detached from the underlying scale, forming isolated wrinkles over the sample surface, while the rest of the surface is still flat. A plan view of the surface of the scale on the same sample shows more clearly the presence of scale convolutions (Fig. 4b).

After oxidation at 700°C (Figs. 5a-5b), ORMA Co-50Cu forms more complex scales including two main regions. The external region is lighter and contains a very thin outermost layer of CuO (middle gray) and an inner quite thick and slightly lighter region composed of Cu_2O (light gray) containing some darker precipitates of CoO. This layer is completely filled with oxide only at relatively few selected places, while at most locations it is completely empty, suggesting that the corresponding oxide scale has been lost during polishing, even though a similar effect is rare. The outermost CuO layer is in contact with the underlying Cu_2O region, where this is still existing. Moreover, the interface between the two scale regions is quite flat and regular. The inner scale layer is considerably darker but not uniform, since its external zone is generally lighter and is composed of a mixture of Cu_2O (lighter gray) with a middle-gray phase which contains large amounts of copper and cobalt, with an atomic ration close to 1/1, which could correspond to the double oxide $CuCoO_2$, plus some darker islands of CoO. The inner zone is darker and is mainly composed

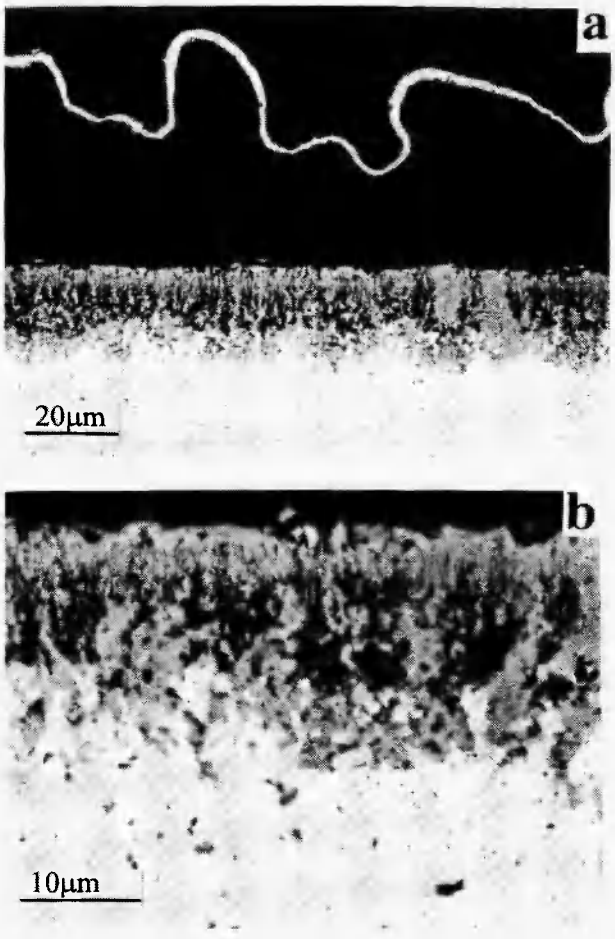

Fig. 3: Micrographs (SEM/BEI) of a cross section of ORMA Co-50Cu oxidized in air at 600°C for 24 h.
(3a) general view;
(3b) expanded view of the inner scale region.

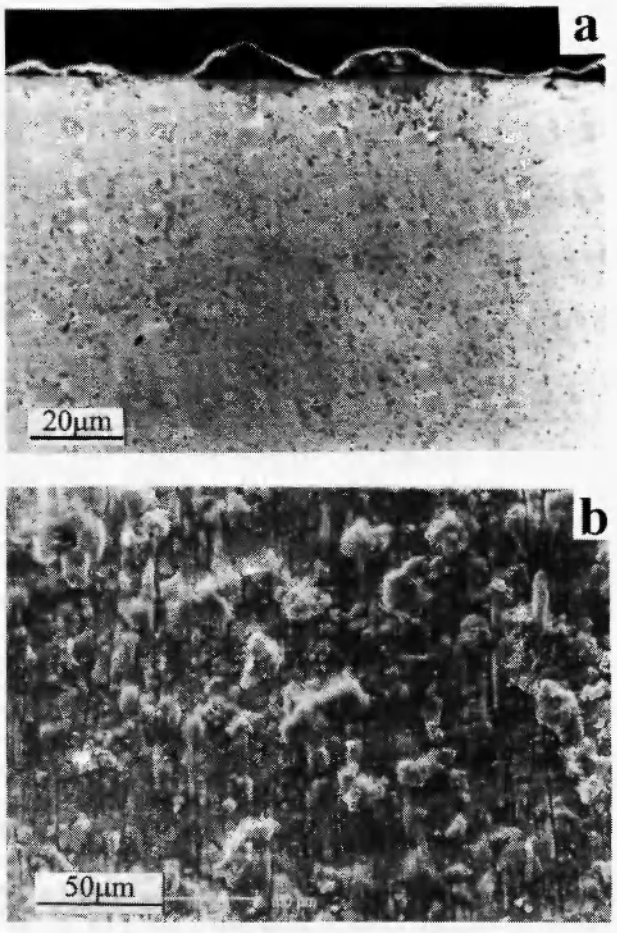

Fig. 4: Micrographs of ORMA Co-50Cu oxidized in air at 600°C for 0.5 h.
(4a) cross section (SEM/BEI);
(4b) surface morphology (SEM/SEI);

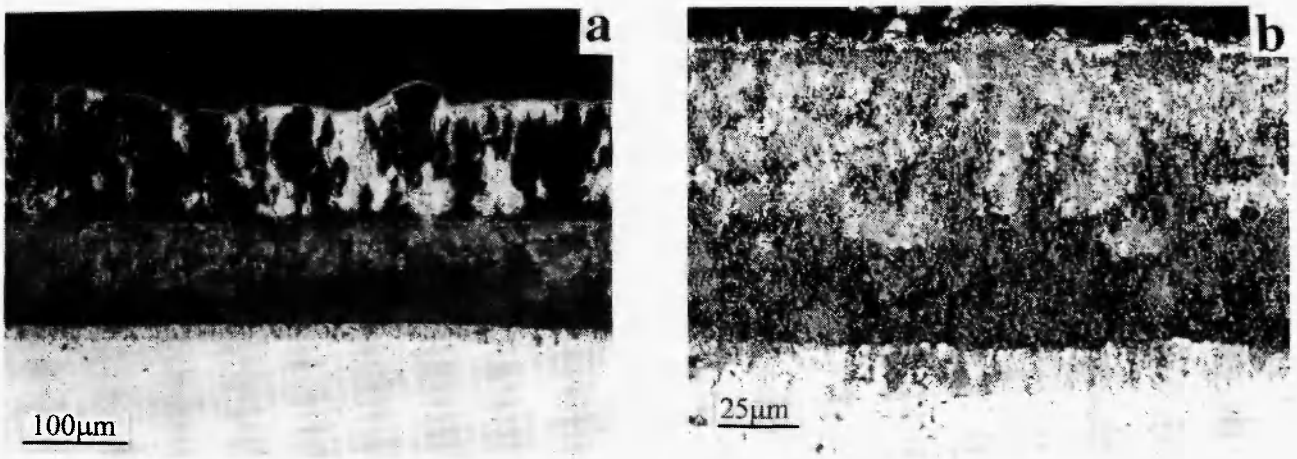

Fig. 5: Micrographs (SEM/BEI) of a cross section of ORMA Co-50Cu oxidized in air at 700°C for 24 h.
(5a) general view;
(5b) expanded view of the inner scale region.

of CoO with some copper in solution (about 3 at%): this zone contains a large number of relatively small but apparently interconnected pores, while the interface between the two zones is quite irregular. Finally, there is also an innermost region of internal oxidation of cobalt.

ORMA Co-50Cu oxidized at 800°C for 24 h (Figs. 6a-6b) contains an external zone composed of many convoluted CuO layers, only partly interconnected, but not in contact with the underlying scale. The inner scale region is much more compact, except for some porous islands (dark), mainly located close to the alloy. The external surface of this layer contains many large light gray outward protrusions, mainly composed of Cu_2O. The remaining fraction of the same layer contains a fine mixture of at least two phases, i.e. Cu_2O and CoO, Cu_2O being lighter than CoO, but possibly also some double Cu-Co oxide. Close to the alloy and above the region of internal oxidation the scale is richer in Cu_2O.

The annealed alloy ANMA Co-50Cu oxidized at 600°C (Fig. 7a) shows a thin outermost CuO layer containing about 8 at% cobalt and an inner layer of CoO

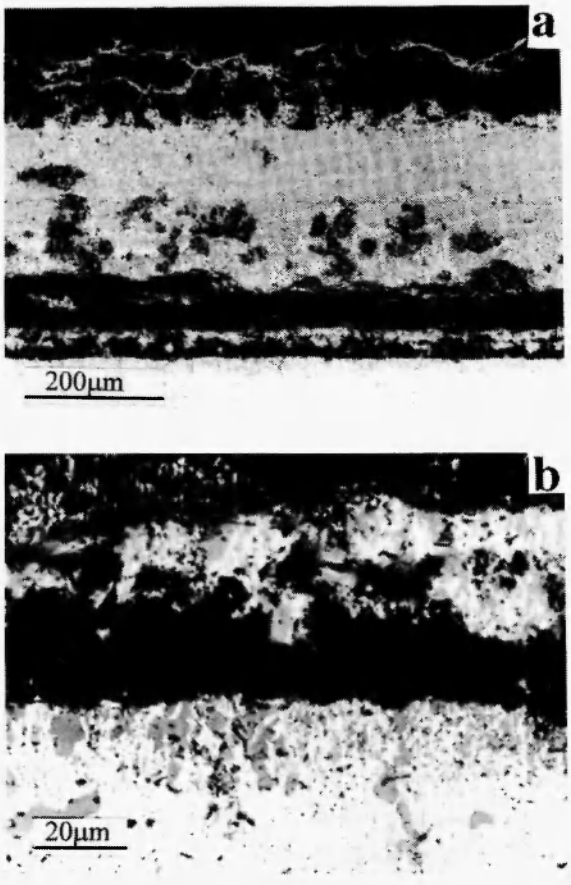

Fig. 6: Micrographs (SEM/BEI) of a cross section of ORMA Co-50Cu oxidized in air at 800°C for 24 h.
(6a) general view;
(6b) expanded view of the inner scale region.

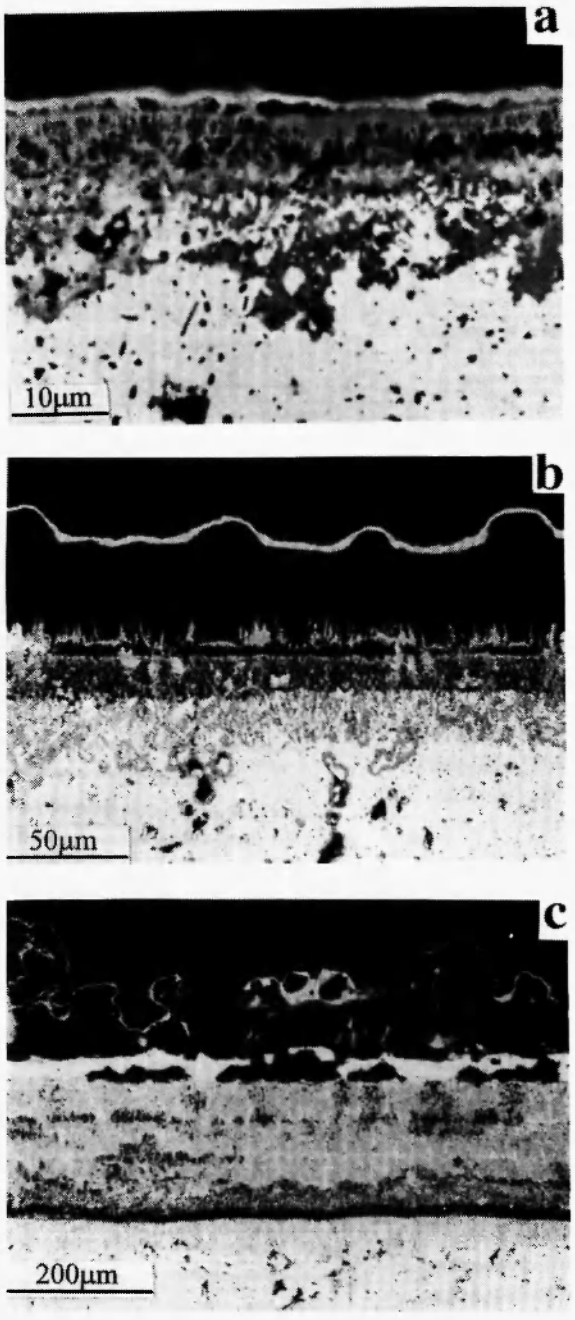

Fig. 7: Micrographs (SEM/BEI) of cross sections of ANMA Co-50Cu oxidized in air for 16 h at 600°C (7a), 700°C (7b) and 800°C (7c).

(gray) with a significant porosity, plus a region of non-uniform depth of internal oxidation of cobalt. At some places the content of copper within the inner CoO layer reaches 13 at%, suggesting the presence of either a mixture of very fine particles of the two oxides or of a double Cu-Co oxide. However, at variance with the ORMA alloy oxidized at the same temperature, the external CuO layer did not convolute but keeps mostly in contact with the underlying scale, since there are only a few holes and/or cracks between this layer and the adjacent scale. After oxidation at 700°C (Fig. 7b), the same alloy shows a wrinkled external layer of CuO, entirely separated from the alloy, at variance with ORMA Co-50Cu at 700°C (Fig. 5a). Beneath this outermost layer, there is a thin irregular layer of Cu_2O containing some cobalt (light), followed by a quite porous layer composed of a fine mixture of Cu_2O and CoO. Finally, there is also a regular region of internal oxidation of cobalt about 25 μm thick, with some large oxide particles deep into the alloy. The scale structure of ANMA Co-50Cu oxidized at 800°C (Fig. 7c) forms an outermost CuO layer containing multi-sublayers, even more convoluted than that at 700°C. The external layer beneath it (light gray) is composed of Cu_2O with 1-2 at% Co in solution, followed by a thick intermediate region composed of a mixture of particles of Cu_2O (light gray) in a darker matrix presenting a large Cu content (about 20 at%), which could correspond either to a fine mixture of CoO with Cu_2O or to a double Cu-Co oxide such as $Cu_xCo_{3-x}O_4$. The distribution of holes in the inner layer is not uniform, since the porosity is larger close to the alloy. Finally, there is a region of internal oxidation of cobalt of regular thickness, which is not in contact with the external scale.

4. DISCUSSION

The oxidation behavior of the present nanophase alloys is rather similar to that of a cast Co-50Cu alloy examined earlier /5/, except for some changes in the oxidation kinetics, especially at 800°C, as well as for the presence of large convolutions in the outermost CuO layer and of large voids in the underlying layer of Cu_2O. These special aspects are examined in detail after considering briefly the general features of the oxidation of the two alloys.

CoO is considerably more stable thermodynamically than Cu_2O, while the oxygen pressures for the Cu_2O/CuO and for the CoO/Co_3O_4 equilibria are very close to each other in the temperature range examined here /5/. Thus Cu_2O can coexist in the scales with CoO, while CuO can coexist with Co_3O_4. In addition, copper and cobalt oxides show some mutual solubility, which is rather large for copper in CoO and form also some double oxides /9,10/. In view of the larger stability of its oxide, cobalt is oxidized preferentially with respect to copper. However, depending mostly on the composition of the bulk alloy, it can either be oxidized internally under external scales of copper oxide, or externally in mixture with copper oxides or finally only externally in the absence of copper oxides (exclusive external oxidation of cobalt) /11,12/. The actual structure of the scales grown on the present alloys corresponds to an internal oxidation of cobalt coupled to the growth of external scales containing a mixture of cobalt and copper oxides, similar to that already observed in the oxidation of normal Co-Cu alloys with a copper content ranging from 25 wt% up to 75 wt% /5/.

The scaling behavior of these alloys can be examined qualitatively using the schematic isothermal phase diagram of the Cu-Co-O system shown in Fig. 8, where, in view of the large difference between the stability of CoO and Cu_2O, the alloy composition for the simultaneous equilibrium with CoO and Cu_2O is assumed to fall inside the field of stability of the α phase. Moreover, P_1 is the oxygen pressure for the equilibria between Cu_2O and CuO and between CoO and Co_3O_4 (assumed to overlap for simplicity), while P_2, P_3, P_4 and P_5 are those for the α-Cu_2O-CoO, pure Cu-Cu_2O, α-β-CoO and pure Co-CoO equilibria, respectively, and $P(O_2)^g$ that prevailing in the gas phase. In the presence of an internal oxidation of cobalt, as observed here, the oxygen pressure prevailing at the front of internal oxidation (P_4) is sufficient to oxidize cobalt, but not copper. Thus, at this site the β phase disappears by reacting with oxygen to form a mixture of CoO and the Co-saturated α phase, while the α phase remains unaffected. At oxygen pressures ranging between P_2 and P_4 the α phase is in equilibrium with CoO but becomes progressively depleted in cobalt by forming new CoO as the oxygen pressures increases in

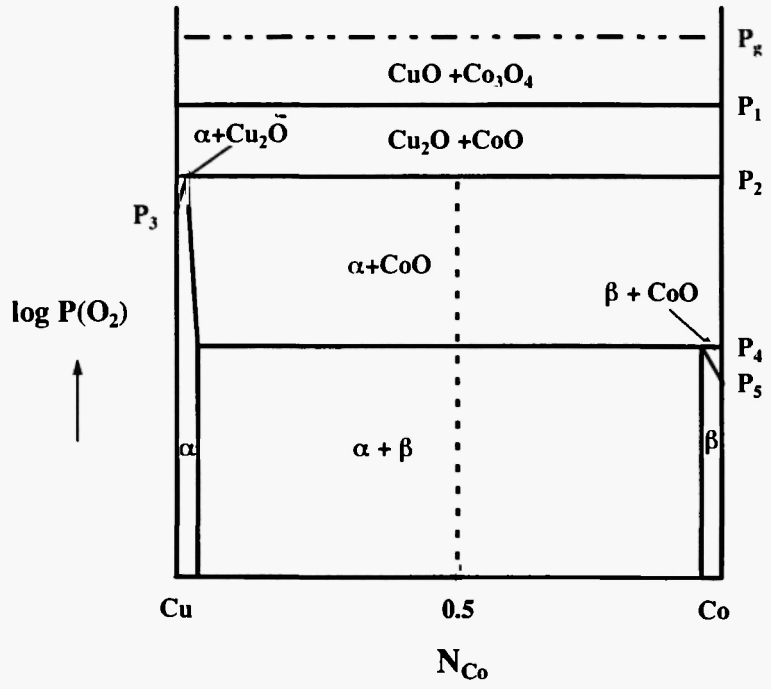

Fig. 8: Schematic isothermal phase diagram for the ternary Co-Cu-O system with an indication of the diffusion path (dashed line) for a Co-50Cu alloy in the region of internal oxidation.

moving outwards through the region of internal oxidation. As for the previous conventional Co-Cu alloys, the diffusion path in the region of internal oxidation of cobalt, i.e. between P_2 and P_4, is essentially a vertical straight line, corresponding to the formation of a mixture of copper metal with CoO, in agreement with what is expected for two-phase alloys presenting a small mutual solubility of the two components /13,14/. Above P_2, also the α phase is oxidized to form Cu_2O, which will form mixtures with the cobalt oxide already formed internally to the alloy. The diffusion path corresponding to the inner region of the external scales (not shown) remains approximately in the same location as for the region of internal oxidation (on the average), but the section corresponding to the outermost scale region is almost completely displaced towards the copper side as a result of the strong local copper enrichment due to the larger rates of growth of copper oxides than cobalt oxides.

For binary solid-solution A-B alloys, a large reduction of the grain size can produce significant changes in the scaling behavior with respect to coarse-grained cast alloys with the same composition, as already observed frequently /15-19 and summarized recently in a study of the high temperature oxidation of a nanophase Cu-10wt%Ni alloy /20/. In fact, the diffusion coefficients of the various species along grain boundaries are generally much larger than through the bulk /21,22/. The faster supply of the B to the alloy/scale interface by diffusion from the interior of the alloy tends to favor the exclusive growth of BO as an external scale by reducing the corresponding critical concentration, as examined in detail elsewhere /20/. This can result also in a significant change in the corrosion kinetics if BO grows at rates much slower than the oxide of A, AO /20/. This situation is typical of alloys containing sufficient amounts of protective elements such as chromium or aluminium to form chromia or alumina scales. For two-phase binary alloys this effect is only possible if the two phases are not in equilibrium in an alloy layer in contact with the scale, and, as a limiting case, if the β phase disappears completely as a consequence of the preferential oxidation of B, leaving a B-depleted α layer /23,24/. In fact, no diffusion of the metal components is possible in the presence of two phases in equilibrium.

Another factor which may favor the formation of external BO scales in the oxidation of binary two-phase alloys composed of a matrix of A-rich α phase containing a dispersion of particles of a B-rich β phase is the size of the β phase particles. In fact, the dissolution of the β phase, essential for an effective supply of B from the alloy to the oxidation front by diffusion through the α phase /23,24/, is faster for small than for large particles under the same overall volume fraction of the β phase as a consequence of the larger value of the surface/volume ratio /25/. This favors the supply of B to the reaction zone, so that small-grained two-phase alloys should present smaller values than the corresponding coarse-grained alloys of the critical B content required for the transition between the formation of mixed external AO + BO scales to the exclusive external oxidation of B. This effect has been observed in the oxidation of two-phase Cu-Cr alloys in air. In fact, alloys with an average grain size of 20-50 μm are not able to form exclusive external chromia scales even for chromium contents up to about 75 wt% by oxidation in air at 700-900°C /26/. On the contrary, Cu-Cr alloys prepared by vapor deposition techniques and presenting a grain size smaller than 1 μm form external chromia scales already at a chromium content of about 25 vol.% when oxidized in air at 650-750°C /27/. In the present case, the exclusive formation of cobalt oxide scales would correspond to a reduction in the rate of oxidation of the two alloys, since the oxidation rate of cobalt is lower than that of copper /6,7/.

The absence of exclusive external oxidation of cobalt in the present alloys is a consequence of their insufficient cobalt content, and in particular of the fact that cobalt is still oxidized internally, thus preventing the formation of a continuous protective CoO layer at the base of the scale. For binary solid-solution A-B alloys presenting the same values as the present materials of the critical factors involved in the internal oxidation of cobalt, including the solubility and diffusivity of oxygen in copper as well as the diffusivity of cobalt in copper, the critical Co content required for the transition between its internal and external oxidation, N(Co)°*, has been calculated as 0.183 at 800°C /5/. The occurrence of an internal oxidation of cobalt in the present alloys in spite of the fact that their cobalt content is much larger than N(Co)°* is then attributed to the presence of two phases, which favors the internal versus the external oxidation of the most reactive component, as predicted /13,14/ and observed in a number of two-phase systems so far /29-33/.

The rate of oxidation of an alloy may still be affected by a reduction of its grain size even when the nature of the scales does not change, as observed in the high-temperature oxidation of a ferritic steel containing 2.25wt% Cr and 1 wt% Mo /34,35/ . In fact, even though no clear relation has apparently been established between the grain size of an alloy and that of the corresponding scales, the scales growing on finer-grained materials also tend to have smaller grains, i.e. to contain a larger concentration of grain boundaries /36-38/. These can affect the rate of scale growth by the same mechanism involved in the mass transport through metallic materials with different grain sizes /11,39-45/. In fact, all reactants diffuse more rapidly along the grain boundaries or other short-circuit paths than through the bulk of the scales, resulting in an acceleration of the scale growth /41,45,46/ which depends again on its grain size and becomes important for fine-grained scales. However, the importance of grain boundary versus bulk transport is generally larger at low than at high temperatures /11,39-46/, contrary to what is observed here. Thus, the increase in the oxidation rate of the nanophase alloys with respect to cast Co-50Cu observed for both alloys at 800°C and for ORMACo-50Cu at 700°C is more likely due to a less protective nature of the corresponding scales, possibly as a result of the presence of a larger amount of porosity or even of cracks, rather than to their smaller grain size.

The main differences in morphology between the scales grown on the nanophase and on the cast Co-50Cu alloys consist in the presence of large convolutions in the outermost CuO layer grown on the small-grained alloys (except for AN Cu-50Co oxidized at 600°C) and of very large voids in the underlying Cu_2O layer, which were absent for the cast alloy. The convolutions of the CuO layer are not caused by the differential thermal contraction on cooling, but develop at temperature since the overall length of this layer is much larger than what can be accounted for by this mechanism /47/. In addition, the outermost layer of the scale grown on MACu-50Co oxidized at 600°C for 0.5 h (Figs. 4a-4b) is less convoluted than that formed after 1 h (Fig. 4c),

and even more than that observed after 24 h, indicating that the oxide ridges form rapidly at temperature and that their size increases with the oxidation time.

The formation of convoluted scales, already observed in the oxidation of many metals and alloys /11,47-49/, has generally been attributed to the presence of compressive stresses in the scale sufficiently large to result in a plastic deformation of the oxide and possibly of the alloy substrate /47,48/. Models to interpret the development of convoluted scales, which apparently acts as a growth-stress relief mechanism, have been proposed by Golightly *et al.* /47/ and by Caplan *et al.* /48/. According to Rhines and Wolf /50/, the compressive stresses result from a coupled diffusion of oxygen inwards and of metal outwards, which produces new oxide within the scale, a process denoted as lateral oxide growth /50/. Eventually, the mechanical stresses become so large as to produce a localized or even complete detachment and buckling of the scale and possibly also the development of cavities between the detached layer and the substrate /51/.

According to the previous mechanism, the main factor involved in the formation of the convoluted external CuO layer on the present alloys would be the inward diffusion of oxygen along the oxide grain boundaries and its local reaction with copper diffusing outward. This is the result of the presence of large concentrations of grain boundaries in the scales growing on the nanophase alloys, producing an increase of the effective diffusion coefficients of both species. In CuO this may be larger for oxygen than for copper, as observed in the growth of alumina. In fact, although Al ions diffuse much more rapidly than oxygen ions in monocrystalline Al_2O_3, diffusion of oxygen in polycrystalline Al_2O_3 is much faster than in single crystals, while Al diffusion is nearly unaffected /49,52, 53/. The grain boundaries of CuO can similarly provide very fast short-circuit diffusion paths, allowing a significant inward penetration of oxygen and generating internal stresses by the previous mechanism. On the contrary, the oxidation of pure copper or of copper-based alloys forming copper oxide scales does not produce convoluted scales /11,20,54,55/, as observed also for the cast Co-Cu alloys /5/, because lattice diffusion of copper in bulk copper oxides is much faster than that of oxygen /11/. Thus, copper oxide scales on large-grained metallic substrates grow almost exclusively at the scale/gas interface by means of an outward diffusion of copper, producing negligible compressive stresses in the scale.

An alternative mechanism for the growth of convoluted scales on the present nanophase alloys is related to the increase of their grain size during exposure at the reaction temperature, as after annealing. The alloy grain growth should also occur during oxidation, but should be more pronounced for the OR than for the AN alloy, since the grain size of ANMACo-50Cu has already increased considerably during annealing. The increase of the grain size involves an increase of the sample density, which can occur by a combination of two processes, i.e. the formation of pores within the sample and a decrease of the overall sample volume. The latter process should also introduce large compressive stresses in the oxide, which may result again in the formation of convoluted scales.

Although the relative importance of the two mechanisms in producing the scale convolutions cannot be established, the contribution of grain boundary diffusion to the overall matter transport through the scale for a given grain size is larger at low than at high temperatures /11,39-46. Thus, if the inward oxygen penetration were the most important mechanism, the convolutions should be larger at 600 than at 800°C, contrary to what was observed. On the contrary, stress generation by a volume contraction of the samples should be larger at high than at low temperatures, and larger for the OR than for the AN alloy. This is also in agreement with the absence of scale convolutions for ANMACo-50Cu oxidized at 600°C, when the increase in the alloy grain size during oxidation should be minimum. Therefore, the decrease of the sample volume due to the increase of its grain size during oxidation seems to be the main factor involved in producing scale convolutions. Finally, both mechanisms can also produce compressive stresses in the underlying compact Cu_2O layer which, with a further contribution from the stresses produced by cooling, can result in an extensive spalling of this oxide layer during polishing rather than producing convolutions. The innermost scale layer is more porous and thus can accommodate stresses more easily without developing spalling or convolutions.

5. CONCLUSIONS

Two Cu-50wt%Co alloys prepared by mechanical alloying and presenting a grain size much smaller than a cast alloy of similar composition showed an oxidation behavior rather similar to that of the cast alloy both for the kinetics and the scale structure, except for faster scaling rates at 700 and 800°C and for the general occurrence of large convolutions of the outermost CuO layer. In all cases, the two alloys formed complex multilayered external scales containing mixtures of the oxides of both alloy components plus an internal oxidation of cobalt. No exclusive external oxidation of cobalt has been achieved, in spite of their rather high cobalt content and of the possibility of a significant increase of the rate of matter transport in the alloy along the grain boundaries present at a large concentration. The large decrease in the grain size of the present nanophase Co-Cu alloys with respect to a coarse-grained cast Co-50Cu alloy is not sufficient to suppress the internal oxidation of cobalt, which is a fundamental requirement for the transition to its exclusive external oxidation. The scale convolutions are attributed to the development of large compressive stresses due more to a volume contraction of the samples associated with an increase of their grain size during oxidation than to a lateral growth of the outermost oxide layer on these materials.

ACKNOWLEDGMENTS

Financial support of this work by the Italian CNR through the PF MSTA-II N. 97.00938.PF34, by the NSFC (No. 59871050-59725101) and by the Italian MURST under the Project "Leghe e Composti Intermetallici: Stabilità termodinamica, proprietà fisiche e reattività" is gratefully acknowledged. One of us (Y.N) is also grateful to CAS-CNR for supporting an exchange visit in 1999 through a collaboration agreement.

REFERENCES

1. T.B. Massalski (Ed.), *Binary Alloys Phase Diagrams*, ASM, USA, 1990.
2. R.H. Yu, J. Zhu, X.X. Zhang and M. Knobel, *Mater. Sci. and Technol.*, **12**, 464 (1996)
3. J.R. Groza and J.C. Gibeling, *Mater. Sci. and Engin.*, A **171**, 115 (1993).
4. M.M. Dadras and D.G. Morris, *Scripta Mat.*, 38, 199 (1998).
5. Y. Niu, J. Song, F. Gesmundo, G. Farn', G. Fu and C. Zeng, *Corros. Sci.*, in press.
6. F. Gesmundo, C. de Asmundis and S. Merlo, *Werkst. und Korros.*, **30**, 114 (1979).
7. F. Morin and M. Rigaud, *Can. Met. Quart.*, **9**, 521 (1970).
8. I. Barin, *Thermochemical Data of Pure Substances,* VCH, Weinheim (FRG), 1989.
9. E.M. Levin, *Phase Diagrams for Ceramists,* American Ceramic Society, Columbus, OH, USA, 1975.
10. R.S. Roth, *Phase Diagrams for Ceramists*, Vol. VI, American Ceramic Society, Westerville, OH, USA, 1987.
11. P. Kofstad, *High Temperature Corrosion*, Elsevier Applied Science, New York, 1988.
12. F. Gesmundo and Y. Niu, *Oxid. Met.*, **50**, 1 (1998).
13. F. Gesmundo, F. Viani and Y. Niu, *Oxid. Met.*, **45**, 51 (1996).
14. F. Gesmundo, F. Viani and Y. Niu, *Oxid. Met.*, **47**, 355 (1997).
15. M.K. Hossain, Corros. *Sci.*, **19**, 1031 (1979).
16. M.D. Merz, *Met. Trans. A*, **10A**, 71 (1979).
17. G.J. Yurek, D.B. Noble and A.J. Garrat-Read, *Proc. 9th International Congress on Metallic Corrosion*, National Reseah Council of Canada, Ottawa, 1984, Vol. II, p. 649.
18. J.G. Goedjen and D.A. Shores, *Oxid. Met.*, **37**, 125 (1992).
19. F.H. Stott, *Materials Characterization*, **28**, 311 (1992).
20. Y. Niu, F. Gesmundo, G. Farné, Y.S. Li, P. Matteazzi and G. Randi, submitted for publication.
21. A. Atkinson, *Solid State Ionics*, **12**, 309 (1984).
22. E.W. Hart, *Acta Met.*, **5**, 597 (1957).
23. F. Gesmundo, F. Viani and Y. Niu, *Oxid. Met.*, 42, 409 (1994).
24. F. Gesmundo, Y. Niu and F. Viani, *Oxid. Met.*, 43, 379 (1995).
25. G. Wang, B. Gleeson and D.L. Douglass, *Oxid.*

Met., **35**, 333 (1991).
26. J. Philibert, *Atom Movements, Diffusion and Mass Transport in Solids*, Les Editions de Physique, Les Ulis (France), 1991, Chapt. X.
27. Y. Niu, F. Gesmundo, F. Viani and D.L. Douglass, *Oxid. Met.*, **48**, 357 (1997).
28. K.T. Chiang, G.H. Meier and F.S. Pettit, *Microscopy of Oxidation-3*, S.B. Newcomb and J.A. Little (Eds.), The Institute of Materials, London, 1997, p. 453.
29. Y. Niu, F. Gesmundo, F. Viani and W.T. Wu, *Oxid. Met.*, **47**, 21 (1997).
30. Y. Niu, F. Gesmundo, D.L. Douglass and F. Viani, *Oxid. Met.*, **48**, 357 (1997).
31. Y. Niu, R.Y. Yan, W.T. Wu F. Gesmundo and G.Y. Fu, *Oxid. Met.*, **49**, 91 (1998).
32. F. Gesmundo, Y. Niu, D. Oquab, C. Roos, B. Pieraggi and F. Viani, *Oxid. Met.*, **49**, 115 (1998).
33. W.T. Wu, G.Y. Fu, Y. Niu and F. Gesmundo, *High Temp. Mater. and Proc.*, **18**, 159 (1999).
34. R.K.S. Raman, A.S. Khanna, R.K. Tiwari and J.B. Gnanamoorthy, *Oxid. Met.*, **37**, 1 (1992).
35. R.K. Singh Raman, J.B. Gnanamoorthy and S.K. Roy, Oxid. Met., **42**, 335 (1994).
36. F. Wang, H. Lou, S. Zhu and W.T. Wu, *Oxid. Met.*, **45**, 39 (1996).
37. F. Wang, *Oxid. Met.*, **47**, 247 (1997).
38. F. Wang, *Oxid. Met.*, **48**, 215 (1997).
39. A. Atkinson, M.L. R.I. Taylor and A.E. Hughes, *Phil. Mag. A*, **45**, 823 (1982).
40. A. Atkinson, M.L. Dwyer and R.I. Taylor, *J. Mater. Sci.*, **18**, 2371 (1983).
41. A. Atkinson, *Rev. Mod. Phys.*, **57**, 437 (1985).
42. A. Atkinson, *Phil. Mag. B*, **55**, 637 (1987).
43. A. Atkinson, in: *Oxidation of Metals and Associated Mass Transport*, M.A. Dayananda, S.J. Rothman and W.E. King (eds.), The Metallurgical Soc., Warrendale , 1987, p. 29.
44. A. Atkinson, Mater. *Sci. Technol.*, **4**, 1046 (1988).
45. A. Atkinson and D.W. Smart, *J. Electrochem. Soc.*, **135**, 2886 (1988).
46. G.J. Yurek, in: *Corros.Mechanisms*, F. Mansfeld (ed.), Marcel Dekker, New York, 1987, p. 397.
47. F.A. Golightly, G.C. Wood and F.H. Stott, *Oxid. Met.*, **14**, 217 (1980).
48. D. Caplan and G.I. Sproule, *Oxid. Met.*, 9, 459 (1975).
49. H. Hindam and D.P. Whittle, *Oxid. Met.*, **18**, 245 (1982).
50. F.N. Rhines and J.S. Wolf, *Met. Trans.*, **1**, 1701 (1970).
51. F.A. Golightly, G.C. Wood and F.H. Stott, *Oxid. Met.*, **10**, 163 (1976).
52. F.A. Kroger, in: *High Temperature Corrosion*, R.A. Rapp (ed.), NACE, Houston, 1983, p. 89.
53. F.H. Stott, *Rep. Progr. Phys.*, **50**, 861 (1987).
54. D.P. Whittle and G.C. Wood, *Corros. Sci.*, **8**, 289 (1968).
55. R. Hausgrud and P. Kofstad, *Oxid. Met.*, **50**, 189 (1998).